

# A description of the Galactic Center excess in the Minimal Supersymmetric Standard Model

---

**Abraham Achterberg,<sup>a</sup> Simone Amoroso,<sup>e</sup> Sascha Caron,<sup>a,b</sup> Luc Hendriks,<sup>a</sup> Roberto Ruiz de Austri,<sup>c</sup> Christoph Weniger<sup>d</sup>**

<sup>a</sup>*Institute for Mathematics, Astrophysics and Particle Physics, Faculty of Science, Mailbox 79, Radboud University Nijmegen, P.O. Box 9010, NL-6500 GL Nijmegen, The Netherlands*

<sup>b</sup>*Nikhef, Science Park, Amsterdam, The Netherlands*

<sup>c</sup>*Instituto de Física Corpuscular, IFIC-UV/CSIC, Valencia, Spain*

<sup>d</sup>*GRAPPA, University of Amsterdam, The Netherlands*

<sup>e</sup>*Albert Ludwigs University Freiburg, Freiburg, Germany*

*E-mail:* [scaron@cern.ch](mailto:scaron@cern.ch), [a.achterberg@astro.ru.nl](mailto:a.achterberg@astro.ru.nl),  
[simone.amoroso@cern.ch](mailto:simone.amoroso@cern.ch), [luc.hendriks@gmail.com](mailto:luc.hendriks@gmail.com), [r Ruiz@ific.uv.es](mailto:r Ruiz@ific.uv.es),  
[c.weniger@uva.nl](mailto:c.weniger@uva.nl)

**ABSTRACT:** Observations with the Fermi Large Area Telescope (LAT) indicate an excess in gamma rays originating from the center of our Galaxy. A possible explanation for this excess is the annihilation of Dark Matter particles. We have investigated the annihilation of neutralinos as Dark Matter candidates within the phenomenological Minimal Supersymmetric Standard Model (pMSSM). An iterative particle filter approach was used to search for solutions within the pMSSM. We found solutions that are consistent with astroparticle physics and collider experiments, and provide a fit to the energy spectrum of the excess. The neutralino is a Bino/Higgsino or Bino/Wino/Higgsino mixture with a mass in the range 84 – 92 GeV or 87 – 97 GeV annihilating into W bosons. A third solution is found for a neutralino of mass 174 – 187 GeV annihilating into top quarks. The best solutions yield a Dark Matter relic density  $0.06 < \Omega h^2 < 0.13$ . These pMSSM solutions make clear forecasts for LHC, direct and indirect DM detection experiments. If the pMSSM explanation of the excess seen by Fermi-LAT is correct, a DM signal might be discovered soon.

**KEYWORDS:** Supersymmetry, MSSM, pMSSM, LHC, Dark Matter

---

## Contents

<b>1</b>	<b>Introduction</b>	<b>1</b>
<b>2</b>	<b>Galactic center observations in light of foreground systematics</b>	<b>3</b>
<b>3</b>	<b>Analysis setup</b>	<b>4</b>
3.1	The Model	4
3.2	Generation and pre-selection of pMSSM model-sets	5
3.3	Parameter scan	6
3.4	Galactic Center excess region	6
<b>4</b>	<b>Results</b>	<b>7</b>
4.1	The galactic center excess	7
4.1.1	WW solution 1: Bino-Higgsino neutralino	7
4.1.2	WW solution 2: Bino-Wino-Higgsino neutralino	9
4.1.3	Top pair solution	10
4.2	Implications for DM direct and indirect experiments	10
4.2.1	WW solution 1: Bino-Higgsino neutralino	11
4.2.2	WW solution 2: Bino-Wino-Higgsino neutralino	12
4.2.3	Top pair solution	13
4.3	Implications for LHC searches	13
4.3.1	WW solution 1: Bino-Higgsino neutralino	13
4.3.2	WW solution 2: Bino-Wino-Higgsino neutralino	14
4.3.3	Top pair solution	14
4.4	Implications for flavour observables	15
<b>5</b>	<b>Discussion</b>	<b>16</b>
<b>A</b>	<b>Uncertainties in the predicted photon spectrum</b>	<b>17</b>

---

## 1 Introduction

Observations of our Galaxy and other individual galaxies [1, 2], clusters of galaxies, gravitational lensing by clusters [3] as well as the detailed properties of the Cosmic Microwave Background [4] all infer that the mass density in the Universe (excluding the vacuum density) is dominated by an unseen component: Dark Matter (DM). Current observational evidence, as well as considerations of standard Big Bang primordial nucleosynthesis, rule out that this unseen component is baryonic in nature, such as a large population of black holes or brown dwarfs [5].

The most likely explanation therefore is that DM consists of a neutral, very weakly interacting particle outside the Standard Model of particle physics, with the currently leading hypothesis being Weakly Interacting Massive Particles (WIMPs) [6–9]. If this particle is a thermal relic, with a mass on the weak scale  $E_w \sim 100$  GeV, the velocity-weighted cross section should be of the order  $\langle\sigma v\rangle \simeq (2 - 5) \times 10^{-26}$  cm<sup>3</sup> s<sup>-1</sup> [10, 11] in order to produce a DM density corresponding to  $\Omega_{\text{DM}} h^2 \simeq 0.12$  as required by observations (e.g. [4]). Here  $\Omega_{\text{DM}}$  is the dark matter density in units of the critical density and  $h = H_0/(100 \text{ km/s per Mpc}) \simeq 0.68$  with  $H_0$  the Hubble constant.

Large-scale simulations of galaxy formation in the context of a flat  $\Lambda$ CDM cosmology all predict extensive, centrally concentrated, dark matter halos around galaxies such as our own [12, 13]. This implies that the strongest possible indirect DM signal should come from the Galactic Center (GC), in particular in the form of gamma rays from DM annihilation (for a recent review see [14]). Gamma rays with photon energies below 100 GeV are not attenuated or deflected during their flight over  $\sim 8.5$  kpc from the GC, unlike other observable decay products [15].

Observations of the GC region with the Fermi-LAT satellite show a gamma ray excess for photon energies that peak in the range  $1 \text{ GeV} \lesssim E_\gamma \lesssim 5 \text{ GeV}$  after a careful (and non-trivial) subtraction of the diffuse emission from known astrophysical sources [16–27]. These include gamma rays due to bremsstrahlung and from the decay of neutral pions produced by cosmic rays in the interstellar gas around the GC. The GC excess extends well away ( $\geq 10^\circ$ ) from the Galactic plane, as expected for a DM signal [24, 28, 29]. Therefore, even though a scenario where the GC excess is caused by conventional sources (e.g. unresolved point sources [30–34] or burst events associated with the  $2 \times 10^6 M_\odot$  central black hole [35, 36]) can not be completely excluded, a DM origin seems not unlikely. Other indirect searches with positrons [37, 38], anti-protons [39–45] or dwarf spheroidal observations [46–49] become increasingly sensitive to the required cross sections.

There have been already a large number of attempts to explain the excess in a plethora of particle physics theories/models [50–100], including supersymmetric (SUSY) [101–114] scenarios [115]. Particular emphasis has been put in SUSY realizations beyond the minimal supersymmetric standard model (MSSM) [82, 91, 116, 117]. The reason is that in the MSSM, the required neutralino annihilation rate to the two golden channels, namely to  $\tau^+\tau^-$  and to  $b\bar{b}$  with neutralino masses of  $\sim 10$  GeV and  $\sim 30$  GeV respectively (as found in most earlier analyses of the excess spectrum) is in tension with LEP or LHC bounds on sfermion masses.

However, recently it has been shown that accounting for systematic uncertainties in the modeling of astrophysical backgrounds [118] opens up the possibility that the annihilation to other final states can fit the excess relatively well, even for DM masses as high as  $\sim 126$  GeV (in the case of  $h^0 h^0$  final states) [115, 119]. This renews the interest in the question of whether the GeV excess can already be accommodated in the MSSM.

In this paper we show how the MSSM offers explanations of the GC excess and how these scenarios are going to be proved in the run II of the LHC and in the near future with the ton-scale DM direct detection experiments and in a complementary way by IceCube with

the 86-strings configuration.

The paper is organized as follows. We describe the uncertainties involved in the GC excess in Section 2. In Section 3 we introduce our theoretical model and the methodology used for its exploration. Section 4 is devoted to present our results and Section 5 for our conclusions. Uncertainties in modelling the photon excess spectrum are discussed in the appendix.

## 2 Galactic center observations in light of foreground systematics

The observed gamma-ray flux from DM annihilation per unit solid angle at some photon energy  $E_\gamma$  is given by

$$\frac{d\Phi_\gamma(E_\gamma)}{dE_\gamma d\Omega} = \frac{\langle\sigma v\rangle}{8\pi m_{\text{DM}}^2} \frac{dN_\gamma}{dE} \int ds \rho_{\text{DM}}^2(r(s, \theta)), \quad (2.1)$$

where the integral is along the line of sight (LOS) at an angle  $\theta$  towards GC,  $\langle\sigma v\rangle$  is the (relative) velocity weighted averaged annihilation cross section,  $m_{\text{DM}}$  denotes the DM mass, and  $dN/dE$  is the photon spectrum per annihilation. The flux is sensitive to uncertainties in the distribution in the radial DM density profile,  $\rho_{\text{DM}}(r)$ , as function of galactocentric distance  $r$ . Dark matter-only simulations of large-scale galaxy formation can in principle resolve the central  $\sim 1\text{--}2$  kpc of DM halo (e.g. [120]). However, for our Galaxy, DM dominates the dynamical estimates for the total (baryonic + DM) enclosed mass,  $M(< r) \sim rV_{\text{rot}}^2/G$ , only beyond a galactocentric distance of 20 kpc, as can be obtained from galaxy rotation curves  $V_{\text{rot}}(r)$ . This renders the inner DM density profile rather uncertain, see for instance [121].

It is quite common to adopt a generalized Navarro, Frenk & White (NFW) profile [12], with  $\rho_{\text{DM}}(r) \propto r^{-\alpha} (r + r_s)^{\alpha-3}$ , with  $\alpha = 1$  for the original NFW profile. The radius  $r_s$  is usually taken to be around 20 kpc, which implies  $\rho_{\text{DM}}^2(r) \propto r^{-2\alpha}$  close to the GC.

The main uncertainties are twofold: (1) Infall of baryonic gas towards the GC in the late stages of galaxy formation initially steepens the DM density profile, increasing  $\alpha$ , while mass loss due to supernova-driven winds from the first generation(s) of massive stars in the Galactic Bulge can flatten it. The net effect is difficult to determine in general, but recent simulations that combine DM with hydrodynamics for the baryonic content [122] show a flattening of the density profile for Milky Way like spiral galaxies (2) The normalization of the DM density distribution is difficult to determine. It is usually parametrized by the DM density at the galactocentric distance of the Sun,  $\rho_{\text{DM}}(r_\odot)$ . Global determinations and local determinations in the Solar neighborhood yield values in the range  $\rho_{\text{DM}}(r_\odot) \simeq 0.2\text{--}0.5 \text{ GeV}/\text{cm}^3$ . The main uncertainties in global determinations stem from modeling of the shape of the halo, while local determinations suffer from uncertainties in the baryonic surface density of the Galactic disk and/or the local stellar kinematics [123, 124].

The consequence for predictions of the flux of the GC excess is that, with particle physics parameters fixed, the uncertainty in the predicted absolute flux level exceeds a factor of a few for realistic parameters. Throughout, we will adopt the estimates of the J-value uncertainty as discussed in [119]. There, the uncertainty of the signal flux at 5 degree distance from the Galactic center was estimated by scanning over a large range of generalized

NFW profiles that are consistent at the 95% CL with the microlensing and rotation curve constraints from [125]. The corresponding J-value uncertainty is (very conservatively, since additional constraints from the slope of the profile in the inner 5 degree are not taken into account) a factor of  $\sim 5$  in both directions.

The existence of a spectrally broad and spatially extended “excess” emission (“Fermi GeV excess”) above conventional convection-reacceleration models for the diffuse gamma-ray emission is by now well established. One of the possible explanations that can explain the properties of this emission surprisingly well is the emission from the annihilation of DM particles.

In order to search for corroborating evidence for the dark matter interpretation of the excess, it is important to estimate the uncertainties of its spectral properties conservatively. We adopt here the results from [118], where the excess emission was studied at latitudes above 2 degree. This region is very sensitive to a dark matter signal, but avoids the much more complicated Galactic center region. The corresponding likelihood function will be discussed below in Section 3.

The MSSM is still the most promising framework for WIMP dark matter models. However, as we will show, it is not completely trivial to find valid model points which provide a spot-on description of the spectrum of the GeV excess. However, in order to not dismiss possible collider signatures that would serve as corroborating evidence for a dark matter interpretation, we will allow below for additional uncorrelated systematics that might affect the spectrum and discuss additional uncertainties e.g. coming from the predictions of the photon energy spectrum from dark matter annihilation, as discussed below. In the case that the DM origin of the GeV excess is supported by other experiments, these additional uncertainties require further study.

### 3 Analysis setup

#### 3.1 The Model

The MSSM has 105 Lagrangian parameters, including complex phases. One can reduce this number to 22 by using phenomenological constraints, which defines the so-called phenomenological MSSM (pMSSM) [126]. In this scheme, one assumes that: (i) All the soft SUSY-breaking parameters are real, therefore the only source of CP-violation is the CKM matrix. (ii) The matrices of the sfermion masses and the trilinear couplings are diagonal, in order to avoid FCNCs at the tree-level. (iii) First and second sfermion generation universality to avoid severe constraints, for instance, from  $K^0 - \bar{K}^0$  mixing. This number can be further simplified to 19 parameters (we will refer to this here as pMSSM) and still capture the phenomenology of the 22-parameter model.

The 19 remaining parameters are 10 sfermion masses,<sup>1</sup> 3 gaugino masses  $M_{1,2,3}$ , the ratio

---

<sup>1</sup>The corresponding sfermion labels are  $\tilde{Q}_1, \tilde{Q}_3, \tilde{L}_1, \tilde{L}_3, \tilde{u}_1, \tilde{d}_1, \tilde{u}_3, \tilde{d}_3, \tilde{e}_1$  and  $\tilde{e}_3$ . Here 1 indicates the light-flavoured mass-degenerate 1st and 2nd generation sfermions and 3 the heavy-flavoured 3rd generation. The labels  $\tilde{Q}$  and  $\tilde{L}$  refer to the superpartners of the left-handed fermionic  $SU(2)$  doublets, whereas the other labels refer to the superpartners of the right-handed fermionic  $SU(2)$  singlets.

of the Higgs vacuum expectation values  $\tan\beta$ , the Higgsino mixing parameter  $\mu$ , the mass  $m_A$  of the CP-odd Higgs-boson  $A^0$  and 3 trilinear scalar couplings  $A_{b,t,\tau}$ .

In this scenario, in principle, there are five arbitrary phases embedded in the parameters  $M_i (i = 1, 2, 3)$ ,  $\mu$  and the one corresponding to the trilinear couplings provided we assume that the trilinear matrices are flavour diagonal. However one may perform a  $U(1)_R$  rotation on the gaugino fields to remove one of the phases of  $M_i$ . We choose the phase of  $M_3$  to be zero. Note that this  $U(1)_R$  transformation affects neither the phase of the trilinear couplings, since the Yukawa matrices being real fixes the phases of the same fields that couple to the trilinear couplings, nor the phase of  $\mu$ . Therefore in the CP-conservation case  $M_1, M_2, \mu$  and the trilinear couplings can be chosen both positive and negative.

### 3.2 Generation and pre-selection of pMSSM model-sets

For our exploration of the pMSSM we use SUSPECT [126] as spectrum generator. DarkSUSY 5.1.1 [127, 128] is used for the computation of the photon fluxes and MicrOMEGAs 3.6.9.2 [129, 130] to compute the abundance of dark matter and  $\sigma_{\chi-p}^{\text{SI}}$  and  $\sigma_{\chi-p}^{\text{SD}}$ .

For the hadronic matrix elements  $f_{T_u}$ ,  $f_{T_d}$  and  $f_{T_s}$ , which enter into the evaluation of the spin-independent elastic scattering cross section we adopt the central values presented in Ref. [131]:  $f_{T_u} = 0.0457$ ,  $f_{T_d} = 0.0457$ . For the strange content of the nucleon we use recently determined average of various lattice QCD (LQCD) calculations  $f_{T_s} = 0.043$  [132]. The spin-dependent neutralino-proton scattering cross-section depends on the contribution of the light quarks to the total proton spin  $\Delta_u$ ,  $\Delta_d$  and  $\Delta_s$ . For these quantities, we use results from a LQCD computation presented in [133], namely  $\Delta_u = 0.787 \pm 0.158$ ,  $\Delta_d = -0.319 \pm 0.066$ ,  $\Delta_s = -0.02 \pm 0.011$  [133] and leave them vary in the  $1\sigma$  range. We will explain why we adopt this approach later.

Following [134], we assume that the ratio of the local neutralino and total dark matter densities is equal to that for the cosmic abundances, thus we adopt the scaling Ansatz

$$\xi \equiv \rho_{\chi}/\rho_{\text{DM}} = \Omega_{\chi}/\Omega_{\text{DM}}. \quad (3.1)$$

For  $\Omega_{\text{DM}}$  we adopt the central value measured by Planck,  $\Omega_{\text{DM}} = 0.1186$  [135]. The photon fluxes are rescaled with  $\xi^2$  when the predicted value is below 0.0938 which encompasses the  $2\sigma$  level uncertainties both in the theoretical prediction and the value inferred by Planck added in quadrature. This allows multi-component Dark Matter.

We select only models with a neutralino as lightest SUSY particle (LSP). From SUSY searchers at colliders we impose the LEP limits on the mass of the lightest chargino. Namely 103.5 GeV [136]. The Higgs mass has been precisely determined by ATLAS and CMS to be 125.4 (ATLAS [137]) and 125.0 GeV (CMS [138]) with uncertainties of 0.3 – 0.4 GeV for each experiment. On top we account for a theoretical error of 3 GeV [139] in its determination and select models with a lightest Higgs boson  $h^0$  within the range:

$$122 \text{ GeV} \leq m_{h^0} \leq 128 \text{ GeV} . \quad (3.2)$$

From the dark matter point of view we in addition demand the following constraints:

- Upper limits from the LUX experiment on the spin-independent cross section [140].

- Upper limits from the IceCube experiment with the 79 string configuration on the spin-dependent cross section [141], assuming that neutralinos annihilate exclusively to  $W^+W^-$  pairs.

In the parameter scan it was required that solutions need to have  $M_A > 800$  GeV or  $5 < \tan(\beta) < 0.075 \cdot M_A - 16.17$  to ensure that they are not excluded by searches for heavy Higgs bosons.

### 3.3 Parameter scan

In a first iteration the pMSSM parameter space was randomly sampled with  $> 10^6$  parameter points from a flat prior. All possible DM annihilation channels have been compared to the measured Fermi photon flux in two energy bins around 1 and 5 GeV. All mass parameters were sampled between  $-4$  TeV and 4 TeV.

In an iterative procedure the best fit points of the first iteration were used as seeds to sample new model parameter ranges centered around the seed points and with multi-dimension Gaussian distribution as widths. The ranges of some parameters were reduced: 100 GeV to 1 TeV and  $-1000$  GeV to  $-100$  GeV for  $M_1$  and  $M_2$ , 100 GeV to 1000 GeV for  $\mu$  and  $\tan\beta$  between 1 and 60. The iterative sampling procedure was repeated several times, until a reasonable annihilation process was found. The process was found to be  $\tilde{\chi}_1^0 \tilde{\chi}_1^0 \rightarrow W^+W^-$  for our first and second solution and  $\tilde{\chi}_1^0 \tilde{\chi}_1^0 \rightarrow t\bar{t}$  for the third solution. The main annihilation diagram is the t-channel exchange of a  $\tilde{\chi}_1^\pm$  (or the t-channel exchange of a stop quark).

In the final iterations 11 of the 19 parameters have been set high enough to be non-relevant (4 TeV). The final set of parameters influence electroweakinos, the Higgs mass and the spin-independent cross section. The final set of parameters was:

$$M_1, M_2, \mu, \tan\beta, M_A, \tilde{d}_3, \tilde{Q}_3, A_t.$$

### 3.4 Galactic Center excess region

For all model points DarkSUSY was used to derive the photon spectrum  $dN/dE$  of the annihilaton process, which was then compared to the spectrum of the GeV excess emission. We adopt the  $\chi^2$  definition from [118], which takes into account correlated uncertainties from the subtraction of Galactic diffuse gamma-ray backgrounds. However, in addition to the astrophysical uncertainties in the measured spectrum as discussed in [118], we allow for an additional 10% uncorrelated uncertainty in the predicted spectrum, as motivated in Appendix A.

We use the following definition

$$\chi^2 = \sum_{i,j} (d_i - m_i)(\Sigma_{ij})^{-1}(d_j - m_j),$$

where  $i$  and  $j$  are the energy bin numbers running from 1 to 24,  $d_i$  and  $m_i$  is the Fermi and model flux, respectively, and  $\Sigma_{ij}$  is the covariance matrix that incorporates all relevant statistical and systematic uncertainties when modeling the GeV excess flux. As mentioned above, we will allow for an additional uncorrelated systematic uncertainty of the level

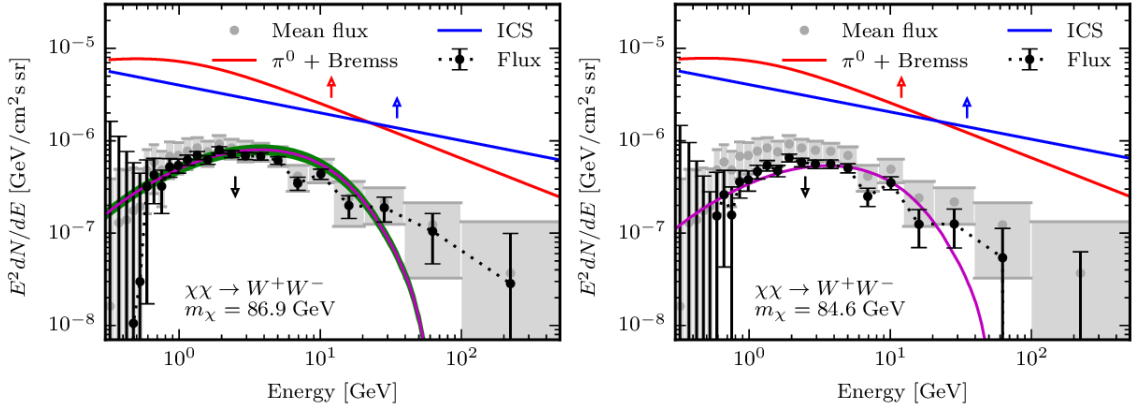


**Figure 1:** Photon excess spectrum as extracted in Ref. [118] from the Fermi data from the inner Galaxy, compared with the model calculations with the lowest  $\chi^2_{10}$  (left figure, p-value= 0.3 with  $\chi^2_{10}$ ) and the model with the lowest  $\chi^2_0$  (right figure, p-value= 0.025 with  $\chi^2_0$ ), for WW solution 1. Note that besides the statistical errors, which are shown as error bars, there are two kinds of systematics which affect the observed photon spectrum (shown as gray dots): Firstly, there are uncertainties from the removal of astrophysical foregrounds (shown by the gray boxes; mostly inverse Compton and  $\pi^0$  emission, see Ref. [118] for details). These uncertainties are strongly correlated and can lead in general to an overall shift of all data points up or down, as illustrated by the black dots. Secondly, there are particle physics uncertainties in the predicted photon spectrum, which we conservatively assume to be at the 10% level (green band in left panel, only affecting  $\chi^2_{10}$ ). Details are discussed in Appendix A.

of  $\sigma_s = 10\%$ , which is incorporated in the covariance matrix from [118] by substituting  $\Sigma_{ij} \rightarrow \Sigma_{ij} + \delta_{ij} d_i^2 \sigma_s^2$ . Photon generation via hadronic  $W^\pm$  or top decays is mainly caused by Quantum Chromo Dynamic processes which are described with semi-empirical models with many parameters. Also the uncertainties in the photon energy scale can change the shape in the modelling of the photon excess spectrum (see Appendix A).

In the following  $\chi^2_0$  denotes  $\sigma_s = 0\%$  and  $\chi^2_{10}$  denotes  $\sigma_s = 10\%$ . Some distributions are shown with both definitions to illustrate the effect of including uncorrelated systematic uncertainties in the predicted photon spectrum.

## 4 Results

### 4.1 The galactic center excess

In our exploration of the pMSSM parameter space we find that requiring a  $\chi^2_{10} < 40$  (corresponding to a p-value  $> 0.02$ ) implies the following three pMSSM parameter ranges:

#### 4.1.1 WW solution 1: Bino-Higgsino neutralino

In this type of solution, the neutralinos annihilate mostly exclusively to  $W^+W^-$  pairs. Only a small fraction annihilate to  $W^+W^-/b\bar{b}$ . The reason is that even being away of the



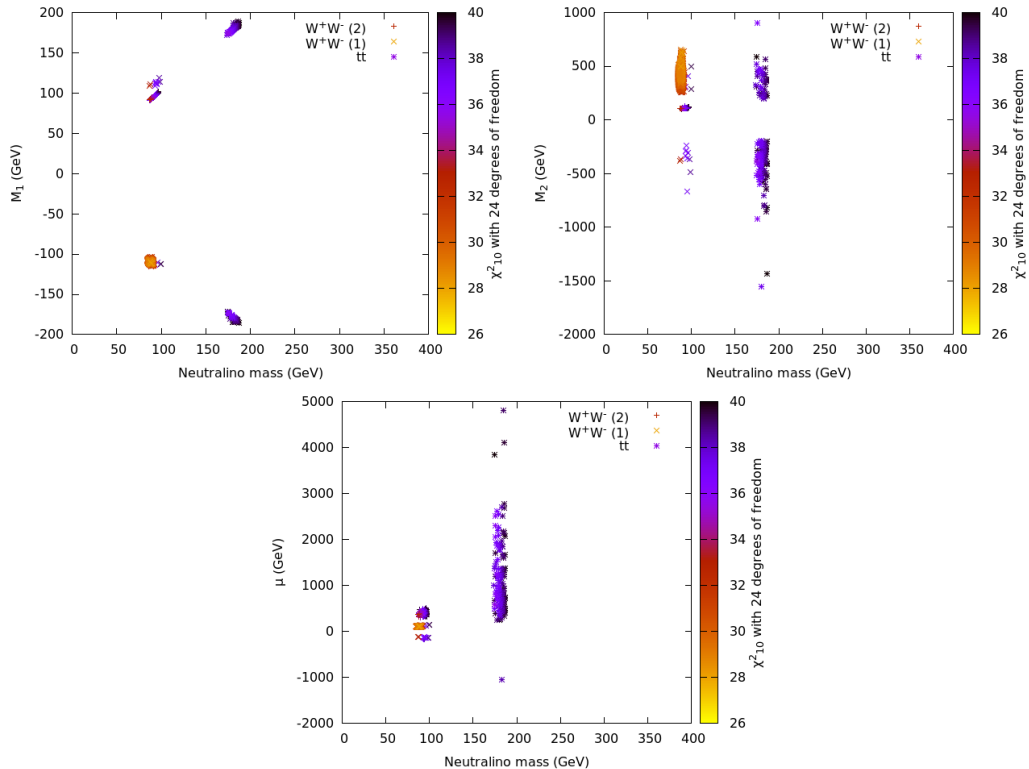


**Figure 2:** The neutralino mass as a function of  $M_1$ ,  $M_2$  and  $\mu$ .  $\chi^2$  is shown as colour code.

A-funnel region the neutralino coupling to pseudoscalars is enhanced due to their bino-higgsino nature and therefore their annihilation to pairs of b-quarks.

This solution provides a good (and in our scan the best) fit to the Galactic center photon spectrum as measured by Fermi. This is partly due to the fact that we, in contrast to previous studies, allow for an additional 10% uncorrelated uncertainty on the predicted photon energy spectrum, as discussed and motivated in Appendix A. The best fit points have  $\chi_{10}^2 \approx 27$  (p-value  $\approx 0.3$ ) with the best-fit normalization of the  $\chi_0^2$ -fit and a  $\chi_{10}^2 \approx 24$  (p-value=0.45) with the best-fit normalization of the  $\chi_{10}^2$ -fit (here we take 10% uncertainties in the predicted spectrum into account in the fit, see above). The best  $\chi_0^2$  was found to be  $\approx 39.5$ . Figure 1 compares the photon spectrum as measured by Fermi with the model calculations with the lowest  $\chi_{10}^2$  and  $\chi_0^2$ .

The properties of these models are shown in Figure 2 (tagged as WW(1)). The best solutions correspond to:

$$-103 \text{ GeV} < M_1 < -119 \text{ GeV},$$

$$240 < M_2 < 660 \text{ GeV},$$

$$108 \text{ GeV} < \mu < 142 \text{ GeV},$$

$$8 < \tan \beta < 50.$$

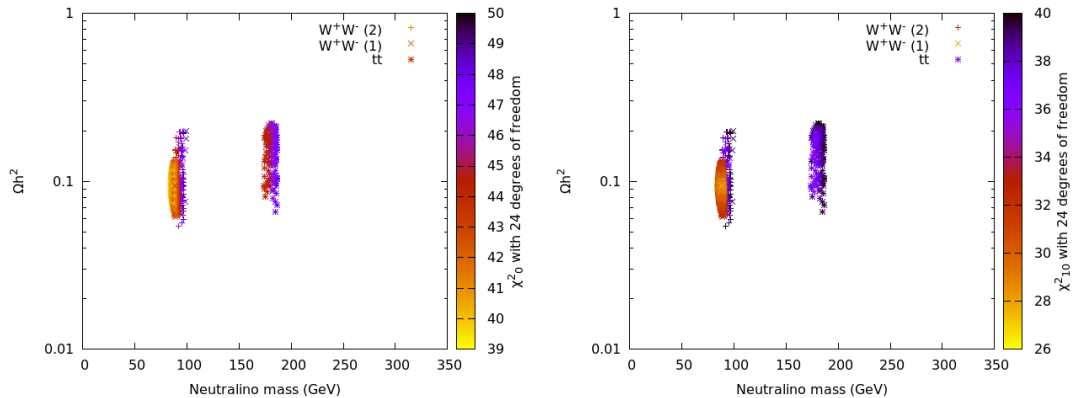


**Figure 3:**  $\Omega h^2$  as a function of the mass of the DM candidate.  $\chi^2$  is shown as colour code. Both  $\chi^2$  definitions are shown.

It can be noticed that the bino mass  $M_1$  and the higgsino mass  $\mu$  are very strictly constrained leading to a precise forecast for DM direct/indirect detection and LHC physics.

The composition of the lightest neutralino is  $\sim 50\%$  bino and  $\sim 50\%$  higgsino and the mass is in the range  $\sim 84 - 92$  GeV.

Figure 3 shows that all points tagged as WW(1) with  $\chi_{10}^2 < 35$  correspond to  $\Omega h^2$  in the range  $\sim 0.07 - 0.125$ . Recall that this constraint was not used in the fit procedure. We consider the outcome as remarkable since  $\Omega h^2$  can vary between  $\approx 10^{-7}$  and  $\approx 10^3$  within pMSSM models.

In terms of constraints coming from electroweakino searches at the LHC  $M_2$  is less tightly constrained and ranges between about 300 – 900 GeV. If  $M_2$  is smaller than about 170 – 250 GeV, the corresponding neutralino (the  $\tilde{\chi}_4^0$ ) decays to  $Z$  and  $\tilde{\chi}_1^0$ . This little part of the valid parameter region is excluded by LHC chargino-neutralino searches already. If  $M_2 > 250$  GeV the  $\tilde{\chi}_4^0$  decays into charginos,  $Z$  and Higgs bosons. This region is not much constrained at the LHC so far. LHC signatures are further discussed in the next section.

Finally, Fig. 5 shows that points consistent with this solution have a pseudoscalar mass  $m_A \gtrsim 350$  GeV, therefore the points that fit well the GC excess lie to the SUSY decoupling regime in which the lightest Higgs is Standard Model like, thus consistent with LHC measurements of the Higgs properties.

#### 4.1.2 WW solution 2: Bino-Wino-Higgsino neutralino

As in the case above, in this type of solution the neutralinos annihilate mostly exclusively to  $W^+W^-$  pairs. The following parameter range yields p-values between 0.02 and 0.15:

$$91 \text{ GeV} < M_1 < 101 \text{ GeV},$$

$$102 \text{ GeV} < M_2 < 127 \text{ GeV},$$

$$156 \text{ GeV} < \mu < 507 \text{ GeV},$$

$$5 < \tan \beta < 12$$

The composition of the neutralino is dominant bino ( $\sim 90\%$ ) with a  $\sim 6\%$  of wino and a  $\sim 4\%$  of higgsino whereas the mass is in the range  $\sim 86.6 - 97$  GeV. Figure 3 shows  $\Omega h^2$  as a function of the mass of the DM candidate (points tagged as WW(2)) with the corresponding  $\chi^2$ . The best fit points have  $0.05 < \Omega h^2 < 0.15$  consistent with Planck.

The LHC sensitivity to this scenario is similar to the Bino-Higgsino case since the only difference is that in this case the neutralinos  $\tilde{\chi}_{3,4}^0$  are heavier than the others. Figure 5 shows, as in the Bino-Higgsino solutions, that the lightest Higgs is “Standard Model like”.

### 4.1.3 Top pair solution

The third solution yields mostly neutralino annihilation into a pair of top quarks via the t-channel exchange of a right-handed stop quark. The neutralino is mostly Bino  $\sim 99\%$  and in this case the chirality suppression in the annihilation cross section that affects to the other fermion final states does not apply here.

As displayed in Figure 2 the solutions (tagged as tt) have a maximum p-value of 0.1. The best solutions imply the following pMSSM parameter range:

$$171 \text{ GeV} < |M_1| < 189 \text{ GeV},$$

$$190 \text{ GeV} < |M_2| < 1550 \text{ GeV},$$

$$\mu > 250 \text{ GeV},$$

$$\tan \beta > 5$$

The neutralino mass is about the kinematical threshold  $m_\chi \sim 174 - 187$  GeV and the right-handed stops have a mass of  $m_{\tilde{t}_1} \sim 200 - 250$  GeV whereas the left-handed are heavy with a mass  $m_{\tilde{t}_2} \sim 2600 - 3700$  GeV to fulfill the Higgs mass constraint.

In this case, as it can be seen Figure 3, all points tagged as tt cover a wider range than in the previous solutions for  $\Omega h^2$  ( $\sim 0.066 - 0.22$ ).

The right-handed stops decay to the lighter chargino and a bottom quark. The chargino is close in mass with the lightest neutralino ( $\Delta \sim 50$  GeV) leading to a hardly visible signal. Therefore this scenario evades current LHC constraints from stop searches.

As above, Figure 5 shows that the pseudoscalar mass  $m_A \gtrsim 500$  GeV, therefore the lightest Higgs is Standard Model like. Figure 8 summarizes the third generation parameters found in the different solutions. The scan localizes very small volume elements of the parameter space.

## 4.2 Implications for DM direct and indirect experiments

**Dwarf spheroidal galaxies** New recent observations of dwarf spheroidal galaxies with the Fermi Large Area Telescope provide by now the most stringent and robust constraints on the velocity-averaged annihilation cross-section [142]. These limits are usually considered have to be taken into account when interpreting the emission seen from the Galactic center in terms of dark matter annihilation. The for us most relevant final states are  $W^+W^-$ ; for a dark matter mass around 80–90 GeV, current upper limits are  $\langle \sigma v \rangle \lesssim 2.6 \times 10^{-26} \text{ cm}^3 \text{ s}^{-1}$  [142].

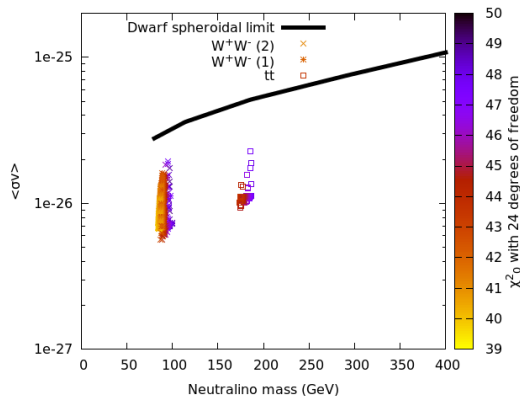


**Figure 4:** The velocity averaged annihilation cross section,  $\langle\sigma v\rangle$  as a function of the mass of the DM candidate.  $\chi^2_{10}$  is shown as colour code. We also show the 95%CL upper limits obtained from a combined observation of dwarf spheroidal galaxies in Ref. [142].

As can be seen from Fig. 4, this constraint is fulfilled by the models considered in this work. In fact, all interpretations presented in this paper require a relatively large J-value at the Galactic center, which implies annihilation cross-sections that are smaller than the thermal value. Hence, although dwarf spheroidal observations could potentially confirm a dark matter interpretation of the GC excess in the future, they cannot currently be used to rule out an interpretation in terms of the MSSM.

**Spin-dependent and spin-independent cross sections** Within the MSSM the dominant contribution to the spin-independent (SI) cross-section amplitude, when squarks are heavy, is the exchange of the two neutral Higgs bosons. The SI cross-section for  $H/h$  exchange is  $\propto |(N_{12} - N_{11} \tan \theta_w)|^2 |N_{13/14}|$ , where  $\theta_w$  is the electroweak mixing angle,  $N_{1i}$  represent the neutralino composition.

With regard to the spin-dependent (SD) cross-section, the dominant contribution corresponds to the exchange of a  $Z$  boson. Since the bino and wino are both  $SU(2)$  singlets, they do not couple to the  $Z$  boson, and therefore SD cross-section is largely determined by the higgsino content of the neutralino. The  $Z$  exchange contribution (and hence the SD cross-section) is proportional to the higgsino asymmetry  $(|N_{13}|^2 - |N_{14}|^2)^2$ . The asymmetry is maximized when either the binos and higgsinos or winos and higgsinos are close in mass.

#### 4.2.1 WW solution 1: Bino-Higgsino neutralino

In solutions of the bino-higgsino type one expects large SI cross-sections as explained above. In fact, the lightest Higgs contribution is effectively fixed and pushes the SI cross-section to values that are in conflict with LUX bounds, therefore cancellations with the heavy Higgs are required. It is well known that these cancellations arise in non-universal models [143]. The degree of cancellation spans the SI cross-section down to  $\sim 10^{-15}$  pb. Those cross sections are going to be probed by ton-scale experiments as Xenon.

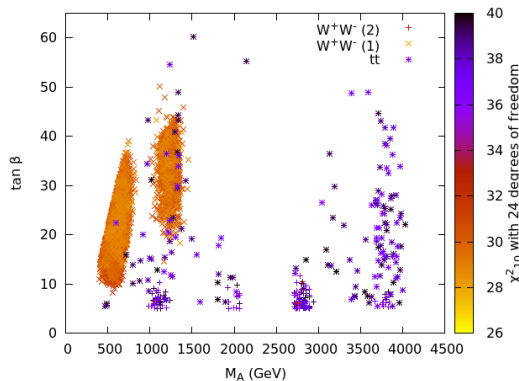


**Figure 5:**  $\chi^2$  (as colour code) for  $M_A$  and  $\tan\beta$ .

This can be seen in the left panel of Figure 6 (points tagged as WW(1)) where we show the  $(\sigma_{\chi-p}^{\text{SI}}, m_\chi)$  plane with the current 90% exclusion limits from the LUX collaboration. The result is rescaled with the scaling Ansatz of Eq. (3.1) to account for the fact that the local matter density might be far less than the usually assumed value local  $\rho = 0.3 \text{ GeV}/\text{cm}^3$ . In the right panel of 6 we display the  $(\sigma_{\chi-p}^{\text{SD}}, m_\chi)$  plane with the current 90% exclusion limits from the IceCube collaboration with the 79 strings configuration assuming that the neutralinos annihilate exclusively to  $W^+W^-$  [141]. Here the SD cross section is not rescaled since the IceCube detection depends on whether the Sun has equilibrated its core abundance between capture rate and annihilation rate. Typically for the Sun, equilibration is reached in our points.

Since the higgsino asymmetry is sizable in this scenario, the SD cross-sections are large and close to the current limits imposed by IceCube. Actually, the model becomes tightly constrained and one has to allow, at least, up  $1\sigma$  deviation of the central values for the hadronic nucleon matrix elements for SD WIMP nucleon cross sections estimated using LQCD. It is interesting to notice that all the currently found points are within the reach of IceCube with the 86 strings configuration. Therefore this phase space is going to be probed in a near future.

#### 4.2.2 WW solution 2: Bino-Wino-Higgsino neutralino

These type of solutions are expected to follow a similar pattern to the Bino-Higgsino scenario. Specially in terms of the SI cross section. This is verified in the left-panel of Figure 6 (points tagged as WW(2)) from where one can infer that ton-scale experiments will probe a sizable fraction of the parameter space consistent with this scenario.

The fact that the Higgsino composition is reduced alleviates the tension in the SD cross section with respect to the current bounds set by IceCube as it can be seen in the right-panel of Figure 6 (points tagged as WW(2)). Indeed we find that all our points are well below the current IceCube limits even taking central values for the hadronic nucleon matrix elements for the SD WIMP nucleon cross sections estimated using LQCD. In terms of prospects most of the points are out of the IceCube reach.

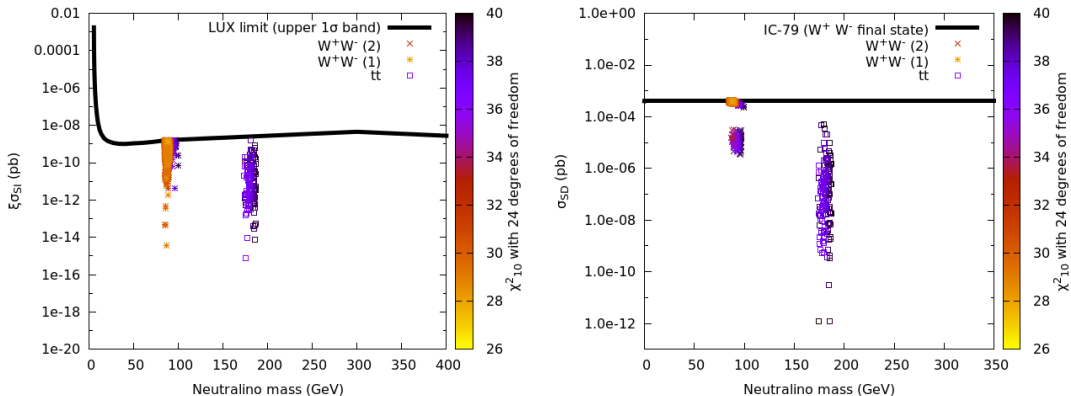


**Figure 6:**  $\sigma_{SI}$  (left-panel) and  $\sigma_{SD}$  (right-panel) as a function of the mass of the DM candidate.  $\chi^2$  is shown as colour code.

### 4.2.3 Top pair solution

With regard to DM detection, points lying to this scenario are expected to have different features with respect to the previous type of solution because the neutralino is mostly bino  $\sim 99\%$ . It leads to a lower prediction for both the SI and SD cross sections as it can be seen in both panels of Figure 6 (points tagged as  $tt$ ). The most evident differences arise in the SD cross section which now expands down to values of  $\sim 10^{-12}$  pb. Clearly this scenario is not going to be fully proved for experiments sensitive, both, to SI and SD cross sections. Despite this, experiments sensitive to the SI cross sections as Xenon 1-ton will probe some fraction of the parameter space consistent with this scenario.

## 4.3 Implications for LHC searches

### 4.3.1 WW solution 1: Bino-Higgsino neutralino

Since the neutralino and chargino mixing matrix parameters are highly constrained in the allowed parameter region the production rates and decays of all neutralinos and charginos are constrained.

Neutralino  $\tilde{\chi}_{1,2,3}^0$  are Higgsinos and Binos, the  $\tilde{\chi}_1^\pm$  is a Higgsino. All these electroweakinos have very similar masses. The decay of the  $\tilde{\chi}_{2,3}^0$  and  $\tilde{\chi}_1^\pm$  to the LSP will not lead to high energetic signals. Consequently the production of the 3 light Neutralinos and the light Chargino will not be visible at LHC in neutralino-chargino searches.

We see a few interesting LHC signals:

**Chargino+Neutralino production.** The only signal visible in electroweakino searches at the LHC could be  $\tilde{\chi}_4^0 \tilde{\chi}^\pm$  production with the subsequent decays of  $\tilde{\chi}_4^0$  to  $Z\tilde{\chi}_1^0$ , Higgs+ $\tilde{\chi}_1^0$  and  $W+\tilde{\chi}_1^\pm$ . Higgs production in this scenario is discussed in [144].

**Monojets.** Since the lightest 3 neutralinos have a similar mass and a Higgsino component they can be pair produced via s-channel  $Z$  production. In addition the  $\tilde{\chi}_1^\pm$  can be produced.

The combined cross sections is enhanced compared to  $\tilde{\chi}_1^0\tilde{\chi}_1^0$  alone. This might lead to a signal in monojet events for the upcoming LHC data.

**Searches for squarks and gluinos.** Finally searches for squarks and gluinos can be conducted in our scenario. If  $M_1, M_2, \mu, \tan\beta$  are fixed, the decays of squarks and gluinos is well determined yielding specific signatures. Especially right-handed squarks will likely decay via the heavy Winos leading again to Z and Higgs signals.

#### 4.3.2 WW solution 2: Bino-Wino-Higgsino neutralino

For this solution Neutralino  $\tilde{\chi}_{1,2}^0$  are mostly Bino-Wino and have a masses of  $\approx 88$  and  $\approx 106$  GeV.  $\tilde{\chi}_1^\pm$  is mostly Wino and has a mass of  $\approx 105$  GeV. On the other side there are 3 heavier states ( $\tilde{\chi}_{3,4}^0$  and  $\tilde{\chi}_2^\pm$ ) with a mass of around 400 GeV.

The LHC signaturs are similar to solution 1:

**Chargino+Neutralino production.** The three heavier states will be visible in the searches for chargino-neutralino production. Again the heavy neutralinos will decay into  $Z\tilde{\chi}_1^0$ , Higgs+ $\tilde{\chi}_1^0$  and  $W+\tilde{\chi}_1^\pm$ .

**Monojets.** Since the lightest 2 neutralinos and the lightest chargino have a similar mass and a Higgsino component they will be visible in monojet production. The cross section will be small compared to solution 1 and the signal will be harder to detect.

**Searches for squarks and gluinos.** For squark and gluino searches the conclusion is similar to solution 1.

#### 4.3.3 Top pair solution

Interesting is that also our third solution seems also not excluded by run-1 LHC searches. The neutralino  $\tilde{\chi}_{1,2}^0$  are again mostly Bino-Wino and have a masses of  $\approx 170$  and  $\approx 225$  GeV.  $\tilde{\chi}_1^\pm$  is mostly Wino and has a mass of  $\approx 225$  GeV. Again we have 3 heavy (dominantly higgsino) states ( $\tilde{\chi}_{3,4}^0$  and  $\tilde{\chi}_2^\pm$ ) with a mass of around 850 GeV.

The solution will lead to the following signatures for run 2:

**Chargino+Neutralino production.** The light neutralino states are again quite compressed and might only be visible with a very soft lepton search.

**Monojets.** The compressed light neutralinos and chargino have masses of  $\approx 170$  GeV which reduces the cross sections for monojet searches compared to the WW scenarios discussed above.

**Search for stops pair production.** The stop mass is  $\approx 230$  GeV. The stop decays 100% to  $\tilde{\chi}_1^\pm$  and a b-jet. The  $\tilde{\chi}_1^\pm$  has a mass difference of  $\approx 50$  GeV with the  $\tilde{\chi}_1^0$ . This signal should be visible with dedicated stop searches in the upcoming run-2 data.

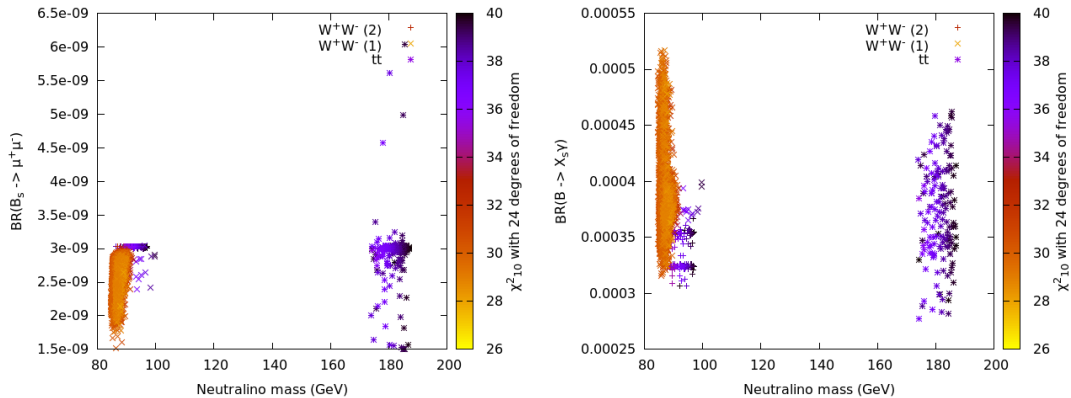


**Figure 7:**  $BR(\bar{B}_s \rightarrow \mu^+ \mu^-)$  (left-panel) and  $BR(\bar{B} \rightarrow X_s \gamma)$  (right-panel) as a function of the mass of the DM candidate.  $\chi^2$  is shown as colour code.

#### 4.4 Implications for flavour observables

Finally in this section we discuss the implications for flavour physics. In Figure 7 we show on the left-panel the  $BR(\bar{B}_s \rightarrow \mu^+ \mu^-)$  and on the right one the  $BR(\bar{B} \rightarrow X_s \gamma)$  versus the neutralino mass.

Accounting for both parametric and theoretical uncertainties in both observables and adding them in quadrature to the experimental ones implies that the allowed range at  $2\sigma$  level is [145]:

$$1.39 \times 10^{-9} < BR(\bar{B}_s \rightarrow \mu^+ \mu^-) < 4.49 \times 10^{-9},$$

$$2.76 \times 10^{-4} < BR(\bar{B} \rightarrow X_s \gamma) < 4.34 \times 10^{-4}.$$

Let us first discuss the  $BR(\bar{B}_s \rightarrow \mu^+ \mu^-)$ : In the left-panel of Figure 7 one can see that all points corresponding to, both, the Bino-Higgsino and Bino-Wino-Higgsino neutralino type of solutions are within the range above. This is quite remarkable since we have not used this observable as constrained in our scan.

In the top pair type of solution the conclusion is broadly the same with the exception of a few points which are ruled out. Those correspond to  $\tan \beta > 40$  where new physics contributions are sizable in the minimal flavour violation scenario [146]. In particular, when stop quarks are relatively light. This is precisely which makes the distinction between the Bino-Higgsino, Bino-Wino-Higgsino neutralino and top pair type of solutions as it has been already pointed out.

In the  $BR(\bar{B} \rightarrow X_s \gamma)$  case, the results are shown in the right-panel of Figure 7. Here a fraction of the points belonging to the Bino-Higgsino neutralino solution are ruled out by current experimental bounds whereas most of points corresponding to both the Bino-Wino-Higgsino and top pair solutions are allowed. The largest values correspond to relatively large  $\tan \beta$  values together with the fact that the lightest chargino is Higgsino like and the interference with the Standard Model contribution is positive since  $sgn(\mu A_t) > 0$  [147]. Again it is worth stressing that most of the solutions are allowed without imposing this constraint in our scan.



## 5 Discussion

We have systematically searched for Dark Matter annihilation processes to explain the excess found in the photon spectrum of the Fermi-LAT satellite. We found three solutions where the excess is explained by the annihilation of neutralinos with a mass around 84 – 92 GeV, 86 – 97 GeV or 174 – 187 GeV.

These solutions yield the following interesting features:

- The neutralino of our first and second solution is a Bino-Higgsino or a Bino-Wino-Higgsino mixture annihilating into  $W^+W^-$ . We obtain a good fit to the Galactic center gamma-ray data by allowing for an additional (and reasonable) uncertainty of the predicted photon spectrum of 10%. The corresponding neutralino and chargino mixing parameters are well constrained for both solutions.
- A third solution is found where a (dominantly Bino) neutralino annihilates into  $t\bar{t}$ , which provides however smaller fit probability for the Galactic center data.
- Since light electroweakinos are compressed, this sector is hard to test at the LHC, but might lead to a signal in monojet (or soft-lepton monojet) events in the upcoming LHC run. In addition the production of the heavy Wino (or mixed) states will be visible for most models.
- Part of the spin-independent cross section can be probed by the upcoming ton-scale direct detection experiments.
- All models points with a Bino-Higgsino neutralino have spin-dependent cross section which are well in the reach of the upcoming spin-dependent constraints provided e.g. by IceCube.
- The best solutions yield values with  $0.06 < \Omega h^2 < 0.13$ . This is a remarkable feature since  $\Omega h^2$  varies for pMSSM solutions unconstrained by the Galactic center excess by about 10 orders of magnitude.

If the MSSM explanation of the excess seen by Fermi-LAT is correct, a DM signal might be discovered soon. The solutions also exist in extensions of the MSSM with a similar stop and electroweakino sector.

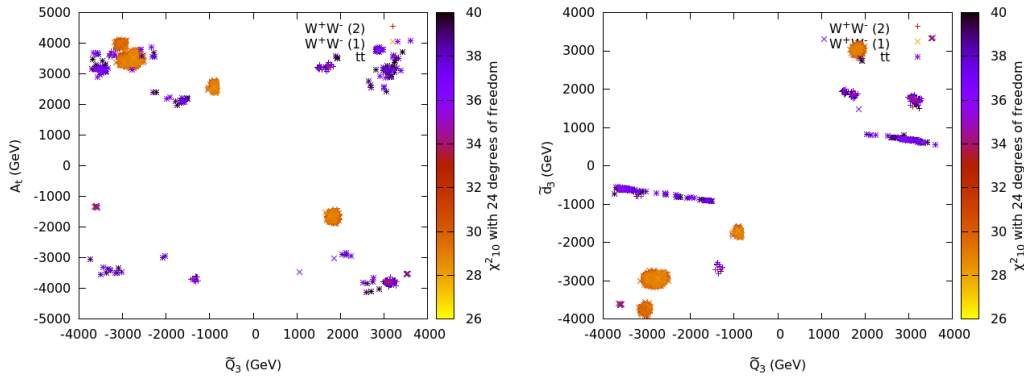


**Figure 8:**  $\chi^2$  (as colour code) for  $\tilde{Q}_3$  and  $A_t$  (left figure). The right figure shows  $\chi^2$  (as colour code) for  $\tilde{Q}_3$  and  $\tilde{d}_3$ .

## A Uncertainties in the predicted photon spectrum

We discuss here briefly sources for uncertainties in the predicted photon spectrum (see [148] for an earlier assessment), and leave a more detailed study to a future publication.

**Generation of the photon spectrum with Pythia.** Dark Matter particles are not charged and cannot directly couple to photons. The Fermi-LAT excess spectrum can be described by Dark Matter (neutralino) annihilation to various SM particles (e.g.  $W^+W^-$  in our models), which then decay further. The decay products can be quarks, which are influenced by the strong force. These quarks can further radiate gluons, which can split into further quarks. This is modelled within Monte Carlo event generators with semi-empirical models (e.g. so called Parton Showering). The quarks are then re-connected to colourless hadrons (again by models based on measurements of fragmentation functions). These hadrons decay and some have significant decay fractions to photons. The photon spectrum is given to a large amount by the momenta and multiplicity distributions of hadrons. By far most important are the decays of neutral particles (mainly  $\pi^0$ ), but photons are radiated at each moment in the chain. The spectrum of photons produced e.g. by  $W^\pm$  decays has never been directly measured down to the energies relevant for the Fermi-LAT spectrum. The generation of a photon spectrum with Monte Carlo event generators has uncertainties stemming from the used model and the model parameters. Here we compare for the same generator and version (Pythia 8.1 [149]) various different fits of the model parameters (see also [150]). The photon spectra are shown in Figure 9 for the annihilation of neutrinos with an energy 85 GeV into  $W^+W^-$ . Besides small effects stemming from the mass of the t-channel propagator the spectrum is identical with the annihilation of a DM particle with a mass 85 GeV into  $W^+W^-$ . The differences range between 5-10% at low photon energies between 0.5-20 GeV and  $\gtrsim 20\%$  at larger energies. This uncertainty should be regarded as a *lower* limit, since no estimate was done to determine the parameter uncertainties via a full extrapolation of data uncertainties. Also no other models (as implemented e.g. in Herwig) have been considered.

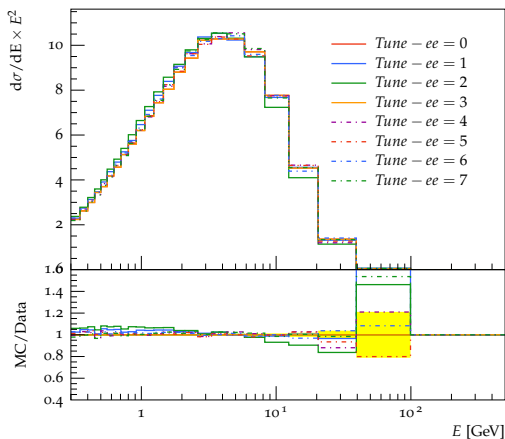


**Figure 9:** Effect of a variation of the Pythia 8 tunes on the generated photon spectrum from  $\nu\bar{\nu} \rightarrow W^+W^-$  with neutrino energies of 85 GeV.

As discussed in the main text, the influence of such additional uncertainties is large: The best-MSSM fit has a p-value of 0.35 including a high-energy physics uncertainty of 10% and p-value of 0.03 without high-energy physics uncertainties.

**Variation of the photon energy scale.** Another significant source of uncertainties is the uncertainty in the photon energy measurement of the Fermi LAT. The photon energy measurement has an uncertainty of 3 – 5% [151] measured in a range  $\approx 6 - 13$  GeV. We assume a  $\pm 1$ -sigma energy measurement uncertainty of  $\pm 5\%$  for the unmeasured region 3–5 GeV as reasonable. We determined the effect on the spectrum by changing the energy of each measured photon by +5% or –5% for all photon energies (and for comparison by  $\pm 10\%$ ).

Figure 10 shows the Pythia generated excess spectrum for neutrino annihilation into  $W^+W^-$  with a neutrino energy of 85 GeV. Nominally, the photon spectrum varies by  $\pm > 5\%$  at energies of  $> 5$  GeV. We conclude that such uncertainties need to be considered in the interpretations of the Fermi excess spectrum. However, we note that a photon energy rescaling does mostly affect the normalization, and not so much the shape of the spectrum. Since the change in the normalization is still much smaller than the uncertainties of the astrophysical J-value, the impact on the fit-quality is in fact not large: Only changing the fit-template from the nominal (no energy variation) to 5% up and 5% down changes  $\chi_0^2$  from 37.8 to 40.4 (up) or 35.3 (down). The p-value changes from 0.035 (nominal) to 0.02 (up) or 0.065 (down).

*Acknowledgements:* R. RdA, is supported by the Ramón y Cajal program of the Spanish MICINN and also thanks the support of the Spanish MICINN’s Consolider-Ingenio 2010 Programme under the grant MULTIDARK CSD2209-00064, the Invisibles European ITN project (FP7-PEOPLE-2011-ITN, PITN-GA-2011-289442-INVISIBLES and the “SOM Sabor y origen de la Materia” (FPA2011-29678) and the “Fenomenologia y Cosmologia de la

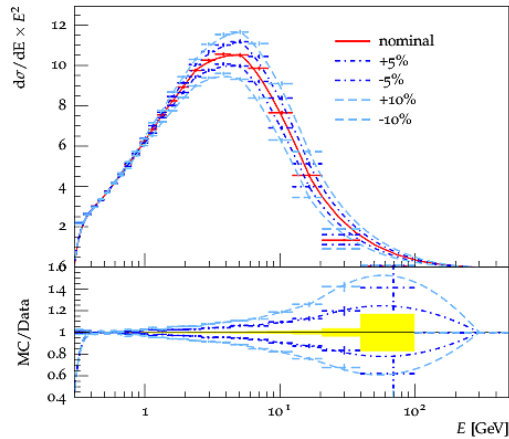


**Figure 10:** Effect of a variation of the photon energy scale by  $\pm 5 - 10\%$  on the generated photon spectrum from  $\nu\bar{\nu} \rightarrow W^+W^-$  with neutrino energies of 85 GeV. Note that the main effect is an overall change in the normalization (which has to be compared with the large uncertainties of the J-value) and a shift of the peak energy in log-space (which can mildly affect the quality of the fit).

Fisica mas alla del Modelo Estandar e Implicaciones Experimentales en la era del LHC” (FPA2010-17747) MEC projects. This work was supported by the Netherlands Organization for Scientific Research (NWO) through a Vidi grant (CW).

## References

- [1] V. C. Rubin, W. K. J. Ford, and N. . Thonnard, *Rotational properties of 21 SC galaxies with a large range of luminosities and radii, from NGC 4605 /R = 4kpc/ to UGC 2885 /R = 122 kpc/, ApJ* **238** (June, 1980) 471–487.
- [2] Y. Sofue and V. Rubin, *Rotation Curves of Spiral Galaxies, Ann. Rev. Astron. Astrophys.* **39** (2001) 137–174, [[astro-ph/0010594](#)].
- [3] D. Clowe, M. Bradač, A. H. Gonzalez, M. Markevitch, S. W. Randall, C. Jones, and D. Zaritsky, *A Direct Empirical Proof of the Existence of Dark Matter, ApJ. L.* **648** (Sept., 2006) L109–L113, [[astro-ph/0608407](#)].
- [4] Planck Collaboration, P. A. R. Ade, N. Aghanim, M. Arnaud, M. Ashdown, J. Aumont, C. Baccigalupi, A. J. Banday, R. B. Barreiro, J. G. Bartlett, and et al., *Planck 2015 results. XIII. Cosmological parameters, ArXiv e-prints* (Feb., 2015) [[arXiv:1502.01589](#)].
- [5] P. Tisserand, L. Le Guillou, C. Afonso, J. N. Albert, J. Andersen, R. Ansari, É. Aubourg, P. Bareyre, J. P. Beaulieu, X. Charlot, C. Coutures, R. Ferlet, P. Fouqué, J. F. Glicenstein, B. Goldman, A. Gould, D. Graff, M. Gros, J. Haissinski, C. Hamadache, J. de Kat, T. Lasserre, É. Lesquoy, C. Loup, C. Magneville, J. B. Marquette, É. Maurice, A. Maury, A. Milsztajn, M. Moniez, N. Palanque-Delabrouille, O. Perdureau, Y. R. Rahal, J. Rich, M. Spiro, A. Vidal-Madjar, L. Vigroux, S. Zylberajch, and EROS-2 Collaboration, *Limits*

- on the Macho content of the Galactic Halo from the EROS-2 Survey of the Magellanic Clouds, *A&A* **469** (July, 2007) 387–404, [[astro-ph/0607207](#)].
- [6] G. Jungman, M. Kamionkowski, and K. Griest, *Supersymmetric dark matter*, *Phys.Rept.* **267** (1996) 195–373, [[hep-ph/9506380](#)].
- [7] G. Bertone, D. Hooper, and J. Silk, *Particle dark matter: Evidence, candidates and constraints*, *Phys.Rept.* **405** (2005) 279–390, [[hep-ph/0404175](#)].
- [8] G. Bertone and J. Silk, *Particle dark matter*, p. 3. Cambridge University Press, 2010.
- [9] L. Bergstrom, *Dark Matter Evidence, Particle Physics Candidates and Detection Methods*, *Annalen Phys.* **524** (2012) 479–496, [[arXiv:1205.4882](#)].
- [10] G. Steigman, *Cosmology confronts particle physics.*, *Annual Review of Nuclear and Particle Science* **29** (1979) 313–338.
- [11] G. Gelmini and P. Gondolo, *DM production mechanisms*, p. 121. Cambridge University Press, 2010.
- [12] J. F. Navarro, C. S. Frenk, and S. D. M. White, *A Universal Density Profile from Hierarchical Clustering*, *ApJ* **490** (Dec., 1997) 493–508, [[astro-ph/9611107](#)].
- [13] M. Boylan-Kolchin, V. Springel, S. D. M. White, A. Jenkins, and G. Lemson, *Resolving cosmic structure formation with the Millennium-II Simulation*, *MNRAS* **398** (Sept., 2009) 1150–1164, [[arXiv:0903.3041](#)].
- [14] T. Bringmann and C. Weniger, *Gamma Ray Signals from Dark Matter: Concepts, Status and Prospects*, *Phys.Dark Univ.* **1** (2012) 194–217, [[arXiv:1208.5481](#)].
- [15] I. V. Moskalenko, T. A. Porter, and A. W. Strong, *Attenuation of Very High Energy Gamma Rays by the Milky Way Interstellar Radiation Field*, *ApJ L.* **640** (Apr., 2006) L155–L158, [[astro-ph/0511149](#)].
- [16] L. Goodenough and D. Hooper, *Possible Evidence For Dark Matter Annihilation In The Inner Milky Way From The Fermi Gamma Ray Space Telescope*, [arXiv:0910.2998](#).
- [17] **Fermi/LAT Collaboration** Collaboration, V. Vitale and A. Morselli, *Indirect Search for Dark Matter from the center of the Milky Way with the Fermi-Large Area Telescope*, [arXiv:0912.3828](#).
- [18] D. Hooper and L. Goodenough, *Dark Matter Annihilation in The Galactic Center As Seen by the Fermi Gamma Ray Space Telescope*, *Phys.Lett.* **B697** (2011) 412–428, [[arXiv:1010.2752](#)].
- [19] D. Hooper and T. Linden, *On The Origin Of The Gamma Rays From The Galactic Center*, *Phys.Rev.* **D84** (2011) 123005, [[arXiv:1110.0006](#)].
- [20] K. N. Abazajian and M. Kaplinghat, *Detection of a Gamma-Ray Source in the Galactic Center Consistent with Extended Emission from Dark Matter Annihilation and Concentrated Astrophysical Emission*, *Phys.Rev.* **D86** (2012) 083511, [[arXiv:1207.6047](#)].
- [21] C. Gordon and O. Macias, *Dark Matter and Pulsar Model Constraints from Galactic Center Fermi-LAT Gamma Ray Observations*, *Phys.Rev.* **D88** (2013) 083521, [[arXiv:1306.5725](#)].
- [22] O. Macias and C. Gordon, *The Contribution of Cosmic Rays Interacting With Molecular Clouds to the Galactic Center Gamma-Ray Excess*, *Phys.Rev.* **D89** (2014) 063515, [[arXiv:1312.6671](#)].

- [23] K. N. Abazajian, N. Canac, S. Horiuchi, and M. Kaplinghat, *Astrophysical and Dark Matter Interpretations of Extended Gamma Ray Emission from the Galactic Center*, [arXiv:1402.4090](#).
- [24] T. Daylan, D. P. Finkbeiner, D. Hooper, T. Linden, S. K. N. Portillo, *et. al.*, *The Characterization of the Gamma-Ray Signal from the Central Milky Way: A Compelling Case for Annihilating Dark Matter*, [arXiv:1402.6703](#).
- [25] B. Zhou, Y.-F. Liang, X. Huang, X. Li, Y.-Z. Fan, *et. al.*, *GeV excess in the Milky Way: Depending on Diffuse Galactic gamma ray Emission template?*, [arXiv:1406.6948](#).
- [26] F. Calore, I. Cholis, and C. Weniger, *Background model systematics for the Fermi GeV excess*, [arXiv:1409.0042](#).
- [27] S. Murgia, *Observation of the high energy gamma-ray emission towards the Galactic center*, 2014. Talk given on Fifth Fermi Symposium, Nagoya, 20-24 October 2014.
- [28] D. Hooper and T. R. Slatyer, *Two Emission Mechanisms in the Fermi Bubbles: A Possible Signal of Annihilating Dark Matter*, *Phys.Dark Univ.* **2** (2013) 118–138, [[arXiv:1302.6589](#)].
- [29] W.-C. Huang, A. Urbano, and W. Xue, *Fermi Bubbles under Dark Matter Scrutiny. Part I: Astrophysical Analysis*, [arXiv:1307.6862](#).
- [30] D. Hooper, I. Cholis, T. Linden, J. Siegal-Gaskins, and T. Slatyer, *Millisecond pulsars Cannot Account for the Inner Galaxy’s GeV Excess*, *Phys.Rev.* **D88** (2013) 083009, [[arXiv:1305.0830](#)].
- [31] F. Calore, M. Di Mauro, and F. Donato, *Diffuse  $\gamma$ -Ray Emission from Galactic Pulsars*, *ApJ* **796** (Nov., 2014) 14, [[arXiv:1406.2706](#)].
- [32] I. Cholis, D. Hooper, and T. Linden, *Challenges in Explaining the Galactic Center Gamma-Ray Excess with Millisecond Pulsars*, [arXiv:1407.5625](#).
- [33] J. Petrovic, P. D. Serpico, and G. Zaharijas, *Millisecond pulsars and the Galactic Center gamma-ray excess: the importance of luminosity function and secondary emission*, [arXiv:1411.2980](#).
- [34] Q. Yuan and B. Zhang, *Millisecond pulsar interpretation of the Galactic center gamma-ray excess*, *JHEAp* **3-4** (2014) 1–8, [[arXiv:1404.2318](#)].
- [35] E. Carlson and S. Profumo, *Cosmic Ray Protons in the Inner Galaxy and the Galactic Center Gamma-Ray Excess*, *Phys.Rev.* **D90** (2014) 023015, [[arXiv:1405.7685](#)].
- [36] J. Petrovic, P. D. Serpico, and G. Zaharijas, *Galactic Center gamma-ray “excess” from an active past of the Galactic Centre?*, *JCAP* **1410** (2014), no. 10 052, [[arXiv:1405.7928](#)].
- [37] L. Bergstrom, T. Bringmann, I. Cholis, D. Hooper, and C. Weniger, *New limits on dark matter annihilation from AMS cosmic ray positron data*, *Phys.Rev.Lett.* **111** (2013) 171101, [[arXiv:1306.3983](#)].
- [38] A. Ibarra, A. S. Lamperstorfer, and J. Silk, *Dark matter annihilations and decays after the AMS-02 positron measurements*, *Phys.Rev.* **D89** (2014) 063539, [[arXiv:1309.2570](#)].
- [39] T. Bringmann, M. Vollmann, and C. Weniger, *Updated cosmic-ray and radio constraints on light dark matter: Implications for the GeV gamma-ray excess at the Galactic center*, [arXiv:1406.6027](#).
- [40] M. Cirelli, D. Gaggero, G. Giesen, M. Taoso, and A. Urbano, *Antiproton constraints on the GeV gamma-ray excess: a comprehensive analysis*, [arXiv:1407.2173](#).

- [41] C. Evoli, I. Cholis, D. Grasso, L. Maccione, and P. Ullio, *Antiprotons from dark matter annihilation in the Galaxy: astrophysical uncertainties*, *Phys.Rev.* **D85** (2012) 123511, [[arXiv:1108.0664](#)].
- [42] I. Cholis, *New Constraints from PAMELA anti-proton data on Annihilating and Decaying Dark Matter*, *JCAP* **1109** (2011) 007, [[arXiv:1007.1160](#)].
- [43] F. Donato, D. Maurin, P. Brun, T. Delahaye, and P. Salati, *Constraints on WIMP Dark Matter from the High Energy PAMELA  $\bar{p}/p$  data*, *Phys. Rev. Lett.* **102** (2009) 071301, [[arXiv:0810.5292](#)].
- [44] R. Kappl and M. W. Winkler, *Dark Matter after BESS-Polar II*, *Phys.Rev.* **D85** (2012) 123522, [[arXiv:1110.4376](#)].
- [45] D. Hooper, T. Linden, and P. Mertsch, *What Does The PAMELA Antiproton Spectrum Tell Us About Dark Matter?*, [[arXiv:1410.1527](#)].
- [46] A. Geringer-Sameth, S. M. Koushiappas, and M. G. Walker, *A Comprehensive Search for Dark Matter Annihilation in Dwarf Galaxies*, [[arXiv:1410.2242](#)].
- [47] I. Cholis and P. Salucci, *Extracting limits on Dark Matter annihilation from gamma-ray observations towards dwarf spheroidal galaxies*, *Phys.Rev.* **D86** (2012) 023528, [[arXiv:1203.2954](#)].
- [48] A. Geringer-Sameth and S. M. Koushiappas, *Exclusion of canonical WIMPs by the joint analysis of Milky Way dwarfs with Fermi*, *Phys.Rev.Lett.* **107** (2011) 241303, [[arXiv:1108.2914](#)].
- [49] **Fermi-LAT Collaboration** Collaboration, A. Abdo *et. al.*, *Observations of Milky Way Dwarf Spheroidal galaxies with the Fermi-LAT detector and constraints on Dark Matter models*, *Astrophys.J.* **712** (2010) 147–158, [[arXiv:1001.4531](#)].
- [50] H. E. Logan, *Dark matter annihilation through a lepton-specific Higgs boson*, *Phys.Rev.* **D83** (2011) 035022, [[arXiv:1010.4214](#)].
- [51] M. R. Buckley, D. Hooper, and T. M. Tait, *Particle Physics Implications for CoGeNT, DAMA, and Fermi*, *Phys.Lett.* **B702** (2011) 216–219, [[arXiv:1011.1499](#)].
- [52] G. Zhu, *WIMPlless dark matter and the excess gamma rays from the Galactic center*, *Phys.Rev.* **D83** (2011) 076011, [[arXiv:1101.4387](#)].
- [53] G. Marshall and R. Primulando, *The Galactic Center Region Gamma Ray Excess from A Supersymmetric Leptophilic Higgs Model*, *JHEP* **1105** (2011) 026, [[arXiv:1102.0492](#)].
- [54] M. Boucenna and S. Profumo, *Direct and Indirect Singlet Scalar Dark Matter Detection in the Lepton-Specific two-Higgs-doublet Model*, *Phys.Rev.* **D84** (2011) 055011, [[arXiv:1106.3368](#)].
- [55] M. R. Buckley, D. Hooper, and J. L. Rosner, *A Leptophobic Z' And Dark Matter From Grand Unification*, *Phys.Lett.* **B703** (2011) 343–347, [[arXiv:1106.3583](#)].
- [56] L. A. Anchordoqui and B. J. Vlcek, *W-WIMP Annihilation as a Source of the Fermi Bubbles*, *Phys.Rev.* **D88** (2013) 043513, [[arXiv:1305.4625](#)].
- [57] M. R. Buckley, D. Hooper, and J. Kumar, *Phenomenology of Dirac Neutralino Dark Matter*, *Phys.Rev.* **D88** (2013) 063532, [[arXiv:1307.3561](#)].
- [58] K. Hagiwara, S. Mukhopadhyay, and J. Nakamura, *10 GeV neutralino dark matter and light stau in the MSSM*, *Phys.Rev.* **D89** (2014) 015023, [[arXiv:1308.6738](#)].

- [59] N. Okada and O. Seto, *Gamma ray emission in Fermi bubbles and Higgs portal dark matter*, *Phys.Rev.* **D89** (2014) 043525, [[arXiv:1310.5991](#)].
- [60] W.-C. Huang, A. Urbano, and W. Xue, *Fermi Bubbles under Dark Matter Scrutiny Part II: Particle Physics Analysis*, *JCAP* **1404** (2014) 020, [[arXiv:1310.7609](#)].
- [61] K. P. Modak, D. Majumdar, and S. Rakshit, *A Possible Explanation of Low Energy  $\gamma$ -ray Excess from Galactic Centre and Fermi Bubble by a Dark Matter Model with Two Real Scalars*, [arXiv:1312.7488](#).
- [62] C. Boehm, M. J. Dolan, C. McCabe, M. Spannowsky, and C. J. Wallace, *Extended gamma-ray emission from Coy Dark Matter*, *JCAP* **1405** (2014) 009, [[arXiv:1401.6458](#)].
- [63] A. Alves, S. Profumo, F. S. Queiroz, and W. Shepherd, *The Effective Hooperon*, [arXiv:1403.5027](#).
- [64] A. Berlin, D. Hooper, and S. D. McDermott, *Simplified Dark Matter Models for the Galactic Center Gamma-Ray Excess*, *Phys.Rev.* **D89** (2014) 115022, [[arXiv:1404.0022](#)].
- [65] P. Agrawal, B. Batell, D. Hooper, and T. Lin, *Flavored Dark Matter and the Galactic Center Gamma-Ray Excess*, *Phys.Rev.* **D90** (2014) 063512, [[arXiv:1404.1373](#)].
- [66] E. Izaguirre, G. Krnjaic, and B. Shuve, *The Galactic Center Excess from the Bottom Up*, *Phys.Rev.* **D90** (2014) 055002, [[arXiv:1404.2018](#)].
- [67] D. Cerden, M. Peiro, and S. Robles, *Low-mass right-handed sneutrino dark matter: SuperCDMS and LUX constraints and the Galactic Centre gamma-ray excess*, *JCAP* **1408** (2014) 005, [[arXiv:1404.2572](#)].
- [68] S. Ipek, D. McKeen, and A. E. Nelson, *A Renormalizable Model for the Galactic Center Gamma Ray Excess from Dark Matter Annihilation*, *Phys.Rev.* **D90** (2014) 055021, [[arXiv:1404.3716](#)].
- [69] C. Boehm, M. J. Dolan, and C. McCabe, *A weighty interpretation of the Galactic Centre excess*, *Phys.Rev.* **D90** (2014) 023531, [[arXiv:1404.4977](#)].
- [70] P. Ko, W.-I. Park, and Y. Tang, *Higgs portal vector dark matter for GeV scale  $\gamma$ -ray excess from galactic center*, *JCAP* **1409** (2014) 013, [[arXiv:1404.5257](#)].
- [71] M. Abdullah, A. DiFranzo, A. Rajaraman, T. M. Tait, P. Tanedo, *et. al.*, *Hidden On-Shell Mediators for the Galactic Center Gamma-Ray Excess*, *Phys.Rev.* **D90** (2014) 035004, [[arXiv:1404.6528](#)].
- [72] D. K. Ghosh, S. Mondal, and I. Saha, *Confronting the Galactic Center Gamma Ray Excess With a Light Scalar Dark Matter*, [arXiv:1405.0206](#).
- [73] A. Martin, J. Shelton, and J. Unwin, *Fitting the Galactic Center Gamma-Ray Excess with Cascade Annihilations*, [arXiv:1405.0272](#).
- [74] T. Basak and T. Mondal, *Class of Higgs-portal Dark Matter models in the light of gamma-ray excess from Galactic center*, [arXiv:1405.4877](#).
- [75] A. Berlin, P. Gratia, D. Hooper, and S. D. McDermott, *Hidden Sector Dark Matter Models for the Galactic Center Gamma-Ray Excess*, *Phys.Rev.* **D90** (2014) 015032, [[arXiv:1405.5204](#)].
- [76] J. M. Cline, G. Dupuis, Z. Liu, and W. Xue, *The windows for kinetically mixed  $Z'$ -mediated dark matter and the galactic center gamma ray excess*, *JHEP* **1408** (2014) 131, [[arXiv:1405.7691](#)].



- [77] T. Han, Z. Liu, and S. Su, *Light Neutralino Dark Matter: Direct/Indirect Detection and Collider Searches*, *JHEP* **1408** (2014) 093, [[arXiv:1406.1181](#)].
- [78] W. Detmold, M. McCullough, and A. Pochinsky, *Dark Nuclei I: Cosmology and Indirect Detection*, [arXiv:1406.2276](#).
- [79] L. Wang, *A simplified 2HDM with a scalar dark matter and the galactic center gamma-ray excess*, [arXiv:1406.3598](#).
- [80] W.-F. Chang and J. N. Ng, *A Minimal Model of Majoronic Dark Radiation and Dark Matter*, *Phys.Rev.* **D90** (2014) 065034, [[arXiv:1406.4601](#)].
- [81] C. Arina, E. Del Nobile, and P. Panci, *Not so Coy Dark Matter explains DAMA (and the Galactic Center excess)*, [arXiv:1406.5542](#).
- [82] C. Cheung, M. Papucci, D. Sanford, N. R. Shah, and K. M. Zurek, *NMSSM Interpretation of the Galactic Center Excess*, *Phys.Rev.* **D90** (2014) 075011, [[arXiv:1406.6372](#)].
- [83] S. D. McDermott, *Lining up the Galactic Center Gamma-Ray Excess*, [arXiv:1406.6408](#).
- [84] J. Huang, T. Liu, L.-T. Wang, and F. Yu, *Supersymmetric Sub-Electroweak Scale Dark Matter, the Galactic Center Gamma-ray Excess, and Exotic Decays of the 125 GeV Higgs Boson*, [arXiv:1407.0038](#).
- [85] C. Balazs and T. Li, *Simplified Dark Matter Models Confront the Gamma Ray Excess*, *Phys.Rev.* **D90** (2014) 055026, [[arXiv:1407.0174](#)].
- [86] P. Ko and Y. Tang, *Galactic center  $\gamma$ -ray excess in hidden sector DM models with dark gauge symmetries: local  $Z_3$  symmetry as an example*, [arXiv:1407.5492](#).
- [87] N. Okada and O. Seto, *Galactic center gamma ray excess from two Higgs doublet portal dark matter*, *Phys.Rev.* **D90** (2014), no. 8 083523, [[arXiv:1408.2583](#)].
- [88] K. Ghorbani, *Fermionic dark matter with pseudo-scalar Yukawa interaction*, [arXiv:1408.4929](#).
- [89] A. D. Banik and D. Majumdar, *Low Energy Gamma Ray Excess Confronting a Singlet Scalar Extended Inert Doublet Dark Matter Model*, [arXiv:1408.5795](#).
- [90] D. Borah and A. Dasgupta, *Galactic Center Gamma Ray Excess in a Radiative Neutrino Mass Model*, [arXiv:1409.1406](#).
- [91] M. Cahill-Rowley, J. Gainer, J. Hewett, and T. Rizzo, *Towards a Supersymmetric Description of the Fermi Galactic Center Excess*, [arXiv:1409.1573](#).
- [92] J. Guo, J. Li, T. Li, and A. G. Williams, *NMSSM Explanations of the Galactic Gamma Ray Excess and Promising LHC Searches*, [arXiv:1409.7864](#).
- [93] M. Freytsis, D. J. Robinson, and Y. Tsai, *Galactic Center Gamma-Ray Excess through a Dark Shower*, [arXiv:1410.3818](#).
- [94] M. Heikinheimo and C. Spethmann, *Galactic Centre GeV Photons from Dark Technicolor*, *JHEP* **1412** (2014) 084, [[arXiv:1410.4842](#)].
- [95] G. Arcadi, Y. Mambrini, and F. Richard, *Z-portal dark matter*, [arXiv:1411.2985](#).
- [96] F. Richard, G. Arcadi, and Y. Mambrini, *Search for Dark Matter at Colliders*, [arXiv:1411.0088](#).
- [97] N. F. Bell, S. Horiuchi, and I. M. Shoemaker, *Annihilating Asymmetric Dark Matter*, *Phys.Rev.* **D91** (2015) 023505, [[arXiv:1408.5142](#)].

- [98] A. Biswas, *Explaining Low Energy gamma-ray Excess from the Galactic Centre using a Two Component Dark Matter Model*, [arXiv:1412.1663](#).
- [99] A. Biswas, D. Majumdar, and P. Roy, *Nonthermal Two Component Dark Matter Model for Fermi-LAT  $\gamma$ -ray excess and 3.55 keV X-ray Line*, [arXiv:1501.02666](#).
- [100] M. J. Dolan, C. McCabe, F. Kahlhoefer, and K. Schmidt-Hoberg, *A taste of dark matter: Flavour constraints on pseudoscalar mediators*, [arXiv:1412.5174](#).
- [101] H. Miyazawa, *Baryon Number Changing Currents*, *Prog. Theor. Phys.* **36** (6) (1966) 1266–1276.
- [102] P. Ramond, *Dual Theory for Free Fermions*, *Phys. Rev.* **D3** (1971) 2415–2418.
- [103] Y. A. Golfand and E. P. Likhtman, *Extension of the Algebra of Poincare Group Generators and Violation of  $p$  Invariance*, *JETP Lett.* **13** (1971) 323–326.
- [104] A. Neveu and J. H. Schwarz, *Factorizable dual model of pions*, *Nucl. Phys.* **B31** (1971) 86–112.
- [105] A. Neveu and J. H. Schwarz, *Quark Model of Dual Pions*, *Phys. Rev.* **D4** (1971) 1109–1111.
- [106] J. Gervais and B. Sakita, *Field theory interpretation of supergauges in dual models*, *Nucl. Phys.* **B34** (1971) 632–639.
- [107] D. V. Volkov and V. P. Akulov, *Is the Neutrino a Goldstone Particle?*, *Phys. Lett.* **B46** (1973) 109–110.
- [108] J. Wess and B. Zumino, *A Lagrangian Model Invariant Under Supergauge Transformations*, *Phys. Lett.* **B49** (1974) 52.
- [109] J. Wess and B. Zumino, *Supergauge Transformations in Four-Dimensions*, *Nucl. Phys.* **B70** (1974) 39–50.
- [110] P. Fayet, *Supersymmetry and Weak, Electromagnetic and Strong Interactions*, *Phys. Lett.* **B64** (1976) 159.
- [111] P. Fayet, *Spontaneously Broken Supersymmetric Theories of Weak, Electromagnetic and Strong Interactions*, *Phys. Lett.* **B69** (1977) 489.
- [112] G. R. Farrar and P. Fayet, *Phenomenology of the Production, Decay, and Detection of New Hadronic States Associated with Supersymmetry*, *Phys. Lett.* **B76** (1978) 575–579.
- [113] P. Fayet, *Relations Between the Masses of the Superpartners of Leptons and Quarks, the Goldstino Couplings and the Neutral Currents*, *Phys. Lett.* **B84** (1979) 416.
- [114] S. Dimopoulos and H. Georgi, *Softly Broken Supersymmetry and  $SU(5)$* , *Nucl. Phys.* **B193** (1981) 150.
- [115] P. Agrawal, B. Batell, P. J. Fox, and R. Harnik, *WIMPs at the Galactic Center*, [arXiv:1411.2592](#).
- [116] J. Cao, L. Shang, P. Wu, J. M. Yang, and Y. Zhang, *SUSY explanation of the Fermi Galactic Center Excess and its test at LHC Run-II*, [arXiv:1410.3239](#).
- [117] D. Cerdeno, M. Peiro, and S. Robles, *Fits to the Fermi-LAT GeV excess with RH sneutrino dark matter: implications for direct and indirect dark matter searches and the LHC*, [arXiv:1501.01296](#).
- [118] F. Calore, I. Cholis, and C. Weniger, *Background model systematics for the Fermi GeV excess*, *ArXiv e-prints* (Aug., 2014) [[arXiv:1409.0042](#)].

- [119] F. Calore, I. Cholis, C. McCabe, and C. Weniger, *A Tale of Tails: Dark Matter Interpretations of the Fermi GeV Excess in Light of Background Model Systematics*, [arXiv:1411.4647](#).
- [120] V. Springel, J. Wang, M. Vogelsberger, A. Ludlow, A. Jenkins, A. Helmi, J. F. Navarro, C. S. Frenk, and S. D. M. White, *The Aquarius Project: the subhaloes of galactic haloes*, *MNRAS* **391** (Dec., 2008) 1685–1711, [[arXiv:0809.0898](#)].
- [121] F. Iocco, M. Pato, and G. Bertone, *Evidence for dark matter in the inner Milky Way*, [arXiv:1502.03821](#).
- [122] P. Mollitor, E. Nezri, and R. Teyssier, *Baryonic and dark matter distribution in cosmological simulations of spiral galaxies*, *MNRAS* **447** (Feb., 2015) 1353–1369, [[arXiv:1405.4318](#)].
- [123] J. Bovy and S. Tremaine, *On the Local Dark Matter Density*, *ApJ* **756** (Sept., 2012) 89, [[arXiv:1205.4033](#)].
- [124] J. I. Read, *The local dark matter density*, *Journal of Physics G: Nuclear and Particle Physics* **41** (2014), no. 6 063101.
- [125] F. Iocco, M. Pato, G. Bertone, and P. Jetzer, *Dark Matter distribution in the Milky Way: microlensing and dynamical constraints*, *JCAP* **1111** (2011) 029, [[arXiv:1107.5810](#)].
- [126] A. Djouadi, J.-L. Kneur, and G. Moultaka, *SuSpect: A Fortran code for the supersymmetric and Higgs particle spectrum in the MSSM*, *Comput.Phys.Commun.* **176** (2007) 426–455, [[hep-ph/0211331](#)].
- [127] P. Gondolo, J. Edsjo, P. Ullio, L. Bergstrom, M. Schelke, *et. al.*, *DarkSUSY: Computing supersymmetric dark matter properties numerically*, *JCAP* **0407** (2004) 008, [[astro-ph/0406204](#)].
- [128] P. Gondolo, J. Edsjo, P. Ullio, L. Bergström, M. Schelke, E. Baltz, T. Bringmann, and G. Duda. <http://www.darksusy.org>.
- [129] G. Belanger, F. Boudjema, A. Pukhov, and A. Semenov, *MicrOMEGAs: A Program for calculating the relic density in the MSSM*, *Comput.Phys.Commun.* **149** (2002) 103–120, [[hep-ph/0112278](#)].
- [130] G. Belanger, F. Boudjema, A. Pukhov, and A. Semenov, *MicrOMEGAs 2.0: A Program to calculate the relic density of dark matter in a generic model*, *Comput.Phys.Commun.* **176** (2007) 367–382, [[hep-ph/0607059](#)].
- [131] X.-L. Ren, L. Geng, J. Martin Camalich, J. Meng, and H. Toki, *Octet baryon masses in next-to-next-to-next-to-leading order covariant baryon chiral perturbation theory*, *JHEP* **1212** (2012) 073, [[arXiv:1209.3641](#)].
- [132] P. Junnarkar and A. Walker-Loud, *Scalar strange content of the nucleon from lattice QCD*, *Phys.Rev.* **D87** (2013), no. 11 114510, [[arXiv:1301.1114](#)].
- [133] **QCDSF Collaboration** Collaboration, G. S. Bali *et. al.*, *Strangeness Contribution to the Proton Spin from Lattice QCD*, *Phys.Rev.Lett.* **108** (2012) 222001, [[arXiv:1112.3354](#)].
- [134] G. Bertone, D. G. Cerdeno, M. Fornasa, R. R. de Austri, and R. Trotta, *Identification of Dark Matter particles with LHC and direct detection data*, *Phys.Rev.* **D82** (2010) 055008, [[arXiv:1005.4280](#)].
- [135] **Planck** Collaboration, P. Ade *et al.*, *Planck 2013 results. XVI. Cosmological parameters*, *Astron.Astrophys.* **571** (2014) A16, [[arXiv:1303.5076](#)].

- [136] **Particle Data Group** Collaboration, K. Olive *et. al.*, *Review of Particle Physics*, *Chin.Phys.* **C38** (2014) 090001.
- [137] **ATLAS** Collaboration, G. Aad *et al.*, *Measurement of the Higgs boson mass from the  $H \rightarrow \gamma\gamma$  and  $H \rightarrow ZZ^* \rightarrow 4\ell$  channels with the ATLAS detector using  $25 \text{ fb}^{-1}$  of  $pp$  collision data*, *Phys.Rev.* **D90** (2014) 052004, [[arXiv:1406.3827](#)].
- [138] **CMS** Collaboration, V. Khachatryan *et al.*, *Precise determination of the mass of the Higgs boson and studies of the compatibility of its couplings with the standard model*, [arXiv:1412.8662](#). CERN-PH-EP-2014-288 ; CMS-HIG-14-009-003.
- [139] B. Allanach, A. Djouadi, J. Kneur, W. Porod, and P. Slavich, *Precise determination of the neutral Higgs boson masses in the MSSM*, *JHEP* **0409** (2004) 044, [[hep-ph/0406166](#)].
- [140] **LUX** Collaboration, D. Akerib *et al.*, *First results from the LUX dark matter experiment at the Sanford Underground Research Facility*, *Phys.Rev.Lett.* **112** (2014) 091303, [[arXiv:1310.8214](#)].
- [141] **IceCube collaboration** Collaboration, M. Aartsen *et. al.*, *Search for dark matter annihilations in the Sun with the 79-string IceCube detector*, *Phys.Rev.Lett.* **110** (2013), no. 13 131302, [[arXiv:1212.4097](#)].
- [142] **Fermi-LAT** Collaboration, M. Ackermann *et. al.*, *Searching for Dark Matter Annihilation from Milky Way Dwarf Spheroidal Galaxies with Six Years of Fermi-LAT Data*, [arXiv:1503.02641](#).
- [143] V. Mandic, A. Pierce, P. Gondolo, and H. Murayama, *The Lower bound on the neutralino nucleon cross-section*, [hep-ph/0008022](#).
- [144] M. van Beekveld, W. Beenakker, S. Caron, R. Castelijns, M. Lanfermann, *et. al.*, *Higgs, di-Higgs and tri-Higgs production via SUSY processes at the LHC with 14 TeV*, [arXiv:1501.02145](#).
- [145] C. Stenge, G. Bertone, G. Besjes, S. Caron, R. Ruiz de Austri, *et. al.*, *Profile likelihood maps of a 15-dimensional MSSM*, *JHEP* **1409** (2014) 081, [[arXiv:1405.0622](#)].
- [146] A. Arbey, M. Battaglia, F. Mahmoudi, and D. Martínez Santos, *Supersymmetry confronts  $B_s \rightarrow \mu^+ \mu^-$ : Present and future status*, *Phys.Rev.* **D87** (2013), no. 3 035026, [[arXiv:1212.4887](#)].
- [147] W. Altmannshofer, M. Carena, N. R. Shah, and F. Yu, *Indirect Probes of the MSSM after the Higgs Discovery*, *JHEP* **1301** (2013) 160, [[arXiv:1211.1976](#)].
- [148] J. Cembranos, A. de la Cruz-Dombriz, V. Gammaldi, R. Lineros, and A. Maroto, *Reliability of Monte Carlo event generators for gamma ray dark matter searches*, *JHEP* **1309** (2013) 077, [[arXiv:1305.2124](#)].
- [149] T. Sjostrand, S. Mrenna, and P. Z. Skands, *A Brief Introduction to PYTHIA 8.1*, *Comput.Phys.Commun.* **178** (2008) 852–867, [[arXiv:0710.3820](#)].
- [150] P. Skands, S. Carrazza, and J. Rojo, *Tuning PYTHIA 8.1: the Monash 2013 Tune*, *Eur.Phys.J.* **C74** (2014), no. 8 3024, [[arXiv:1404.5630](#)].
- [151] **Fermi-LAT** Collaboration, M. Ackermann *et. al.*, *The Fermi Large Area Telescope On Orbit: Event Classification, Instrument Response Functions, and Calibration*, *Astrophys.J.Suppl.* **203** (2012) 4, [[arXiv:1206.1896](#)].